

Configuration Dependency of Attached Epoxy Groups on Graphene Oxide Reduction: A Molecular Dynamics Simulation

To cite this article: Kyung-Han Yun *et al* 2012 *Jpn. J. Appl. Phys.* **51** 06FD14

View the [article online](#) for updates and enhancements.

You may also like

- [Dispersity control and anti-corrosive performance of graphene oxide modified by functionalized nanosilica in waterborne polyurethane](#)
Xiaopeng Zhang, Jie Wen, Baisong Hu et al.
- [First-principles insight into Li and Na ion storage in graphene oxide](#)
Shu-Ying Zhong, Jing Shi et al.
- [Synthesis of borosiloxane oligomers containing vinyl and epoxy groups for improving adhesion of addition-curable silicone rubber with epoxy resin](#)
Yu-Long Zhang, Chong-Guang Zang, Qing-Jie Jiao et al.

Configuration Dependency of Attached Epoxy Groups on Graphene Oxide Reduction: A Molecular Dynamics Simulation

Kyung-Han Yun, Yubin Hwang, Minho Lee, Heechae Choi, Dong Su Yoo,
Eung-Kwan Lee, Sung Beom Cho, and Yong-Chae Chung*

Department of Materials Science and Engineering, Hanyang University, Seoul 133-791, Republic of Korea

Received November 30, 2011; accepted January 13, 2012; published online June 20, 2012

The atomic behavior of epoxy groups on a graphene oxide sheet was observed during high thermal heat annealing using a reactive force-field based on molecular dynamics simulations. We found the oxygen-containing functional groups interplay with each other and desorbed from the graphene oxide sheet by a form of O₂ gas if they were initially in close distance. Through comparing reduction results of graphene oxide with different densities of the nearest neighboring epoxy pairs, we confirmed that the amount of released O₂ gas has a clear tendency to increase with a higher density of epoxy pairs in close distance on a graphene oxide sheet. © 2012 The Japan Society of Applied Physics

1. Introduction

Graphene recently emerged as a new material for electronic devices due to its excellent electrical and optical properties.^{1–8} In the area of graphene fabrications, the most efficient method for its large-scale production is the reduction of graphene oxide (GO), a material that shares the same atomically thin structural framework as graphene, but accompanies oxygen-containing functional groups.^{9–15} Reduced GO still contains residual oxygen atoms that are sp³ bonded to approximately 20% of carbon atoms.^{1,16–18} The remaining oxygen atoms induce the decrease of the mobility of charge carriers.^{19–23} Therefore, for many experts, it has been a challenging task to pick off oxygen atoms from GO sheets and fabricate pristine graphene sheets.^{17,24–27} However, the knowledge about bonding configuration or location of the residual oxygen is insufficient. To meet these requirements, research using molecular dynamics (MD) simulations and density functional theory (DFT) calculations was conducted to observe the chemical reactions of oxygen-containing groups on the annealing of GO on the atomic scale by Bagri *et al.*²⁹ According to an MD simulation study, the epoxy groups problematically require higher energy for desorption than the hydroxyl functional groups, and are likely to still remain on graphene sheet if they are initially isolated.^{28–30}

Although the information about the density and type of defects generated during heat annealing and hybridization states of C–C and C–O bonds and their spatial distribution was satisfied through atomic-scale simulation research, there still remains a lack of understanding of how the oxygen functional groups, such as epoxy, carbonyl and ether, interact with each other during thermal annealing. Thus it is necessary to understand the atomistic behavior of oxygen functional groups through atomic-scale MD simulations to find the factor which plays a crucial role for desorption of these functional groups from a GO sheet.

2. Calculation Methods

Our MD simulations were performed using the Sandia-developed code, large-scale atomic/molecular massively parallel simulator (LAMMPS) and the reactive force-field (ReaxFF)³¹ potential, which is appropriate for elucidating chemical reactions between carbon and oxygen atoms. We

first set the graphene sheet (8.3 × 8.0 nm²) with randomly distributed epoxy functional groups on both sides of the sheet with an initial oxygen concentration of 30% of carbon atoms. According to the supplementary information of the previous MD study, the effects of cell size on the morphology of GO sheets and the distribution of functional groups were negligible.²⁹ In order to exclude the edge effects, we applied periodic boundary conditions along the basal plane of the graphene sheet. Using the isothermal-isobaric (NPT) ensemble with a Berendsen thermostat for temperature control, the system was first heated from 10 to 1,000 K for a time span of 625 fs to find the equilibrated structure of GO, then annealed at 1,000 K for 625 fs, and quenched to a room temperature of 300 K for 625 fs. Finally the GO sheet was annealed at 300 K for 4.25 ps to confirm zero pressure in the plane.

After relaxation of the GO sheet, we switched to the canonical moles (N), volume and temperature (NVT) ensemble. Then, the system was heated from 300 to a typical reduction temperature of 1,500 K for a time span of 250 fs and annealed at that temperature for 75 ps, and quenched to 300 K for 250 fs. After quenching at 300 K, the system was held at that temperature for a time span of 1.25 ps. Every simulation was performed with a time step of 0.25 fs.

In order to confirm the correlation between the initial configuration of epoxy pairs and reduction tendency, we selected three GO models based on the density of the first nearest neighboring epoxy pairs from 1,000 different GO sample sheets. Statistically, the most representative sample is the GO sheet with the number of 171 first nearest neighboring epoxy pairs (44.53%) from a total of 768 oxygen atoms on the GO sheet. The other two samples consist of 143 (37.24%) and 203 (52.86%) first nearest neighboring epoxy pairs.

3. Results and Discussion

We designed GO models, including epoxy functional groups. As shown in Fig. 1(a), the initial epoxy groups are randomly positioned on both sides of the graphene basal plane. Considering the saturated coordination number of each carbon atom (sp³), only one epoxide is set to be located above the middle point of three neighboring C–C bonds. The distances of the first and second nearest epoxy pairs are 2.17 and 2.50 Å, respectively [Fig. 1(b)].

As shown in Fig. 2(a), after relaxation of the GO at room temperature, carbonyls or ether rings were created by

*E-mail address: yongchae@hanyang.ac.kr

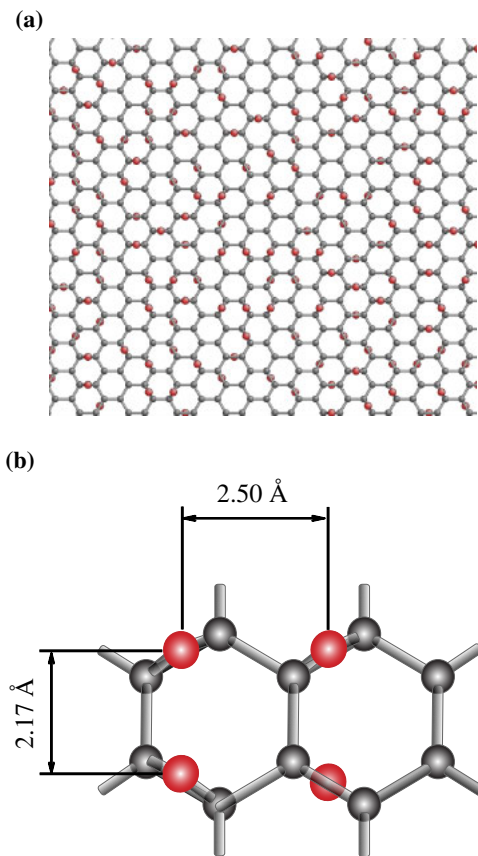


Fig. 1. (Color online) Initial configuration of epoxy on a GO sheet with 30% initial oxygen concentration of carbon atoms. (a) The morphology of GO sheet with 171 first nearest oxygen pairs and (b) the configuration of first and second nearest neighboring oxygen pairs at a distance of 2.17 and 2.50 Å, respectively. Red circles indicate oxygen and carbon is the gray circles.

rearrangement of each epoxy group and surrounded closely by saturated carbon atoms (sp^3). Although the epoxy groups were rearranged, we found that the oxygen atoms were mostly positioned on the same site where they initially were before system equilibration, but there occurred only a C–C bond break due to the strain in neighboring C–C bonds by insufficient non-planar sp^3 -bonding for carbon bonding to oxygen. Figure 2(b) indicates that the carbonyls, ether rings or epoxy groups remained on the GO sheet after relaxation at 300 K.

To understand the mechanism of O_2 evolution, we observed the atomic-scale desorption process of O_2 gas during annealing at 1,500 K. Figures 3(a) and 3(b) show the representative cases of the available desorption process of O_2 gas. We found that the O_2 gas desorbed from the graphene sheet only in three cases of the initial position of carbonyl–carbonyl, carbonyl–epoxy, or carbonyl–ether ring in close proximity and on the same side of the basal plane. There occurred no evolution of O_2 gas when these carbonyl–carbonyl, carbonyl–epoxy, or carbonyl–ether pairs were positioned on the opposite side of the basal plane.²⁹

As shown in the top frame of Fig. 3(a), in the case of a hole with a carbonyl pair, two carbon atoms bonding to oxygen easily move close to each other and make a bond together. After the carbon pair bonds, then the oxygen atoms break one double bond of $C=O$ and form their own bond. As

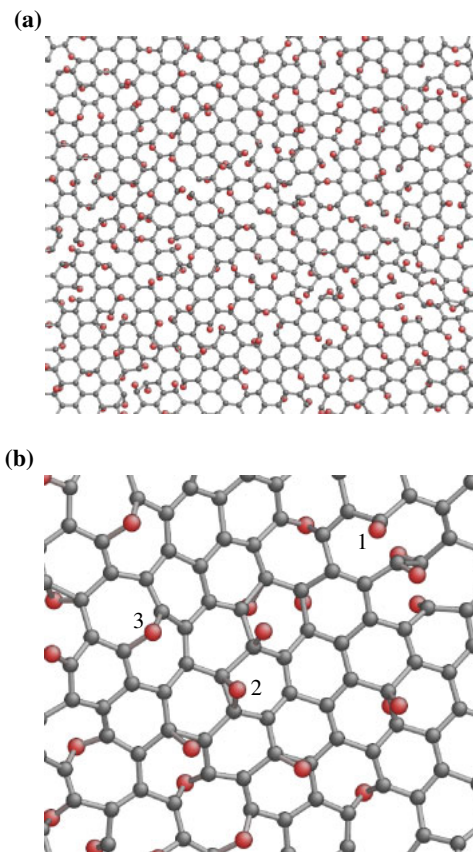


Fig. 2. (Color online) (a) Morphology of GO sheet with 171 first nearest neighboring oxygen pairs after relaxation at room temperature (300 K). (b) Oxygen functional groups formed after annealing: carbonyl (1), epoxy (2), ether (3).

a result of the transition from double to single bond between carbon and oxygen, the oxygen gas desorbs from the graphene sheet with the breaking of a C–O bond. In the case of a carbonyl–ether pair [Fig. 3(b)], as a first step, two carbon atoms bonding with ether (C–O–C) bond together and one of C–O bonds is broken at the same time because it is energetically more favorable for the carbon atoms to make sp^2 hybridization than sp^3 bond including with an oxygen atom.³⁰ Then the oxygen atoms come close to each other and bond due to the frustrated single bond of each oxygen atom. Finally the O_2 gas desorbs from the graphene sheet with the breaking of a relatively weaker bond of C–O than O=O. Figure 3(c) shows the behavior of oxygen atoms during desorption from the carbonyl–epoxy pair configuration. The hole sharing two carbon atoms first makes a bond to return to sp^2 bonding status among them (carbon atoms) and then the dissociated oxygen mono atom moves to the nearest oxygen functional group as indicated in the second frame of Fig. 3(c). After the bonding of oxygen atoms, the O_2 gas desorbs from the graphene sheet as shown in the final step.

The evolution of O_2 gas occurred when oxygen functional group pairs were in close proximity [Figs. 4(a) and 4(b)]. The oxygen functional groups, which were initially isolated from other functional groups or remained after desorption of near oxygen pairs, still remained on the GO sheet. The oxygen pairs encircled were released by a form of O_2 gas after annealing at 1,500 K [Fig. 4(a)]. Besides, the pathways

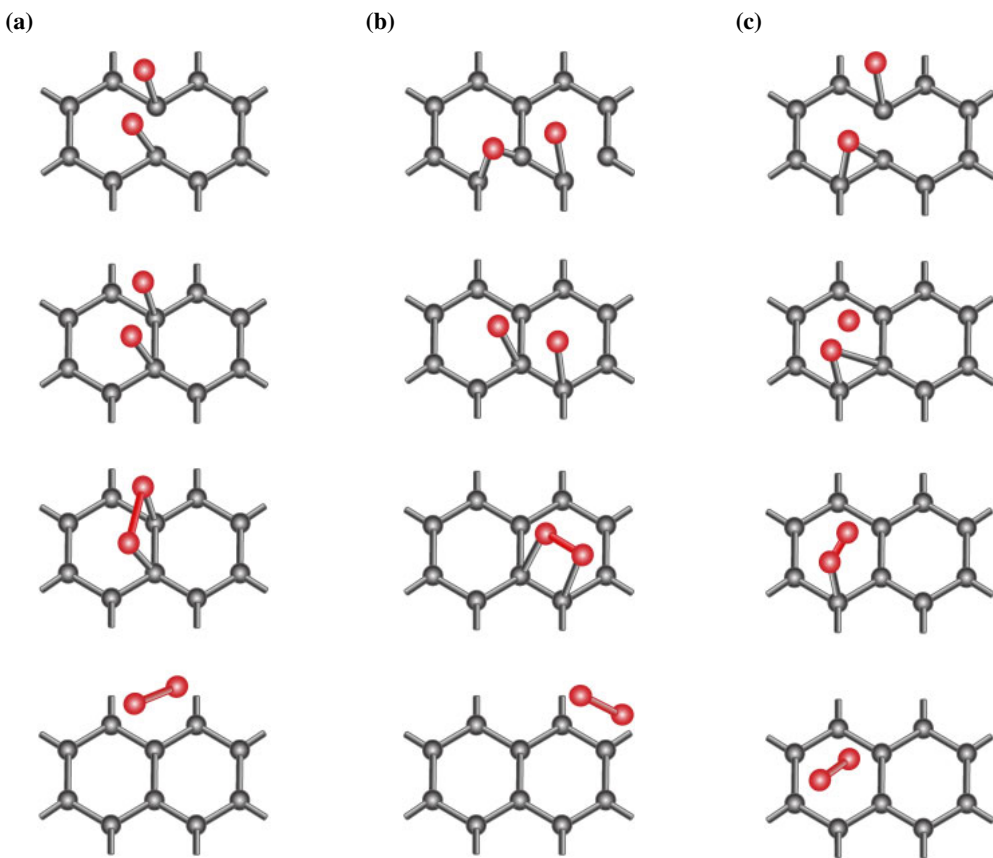


Fig. 3. (Color online) The desorption processes of oxygen atoms during annealing at 1,500 K. (a) The case of carbonyl–carbonyl pair, (b) carbonyl–ether pair, and (c) carbonyl–epoxy pair in close distance on the same side of the GO basal plane. From top to bottom, each frame shows the kinetics of the desorption process.

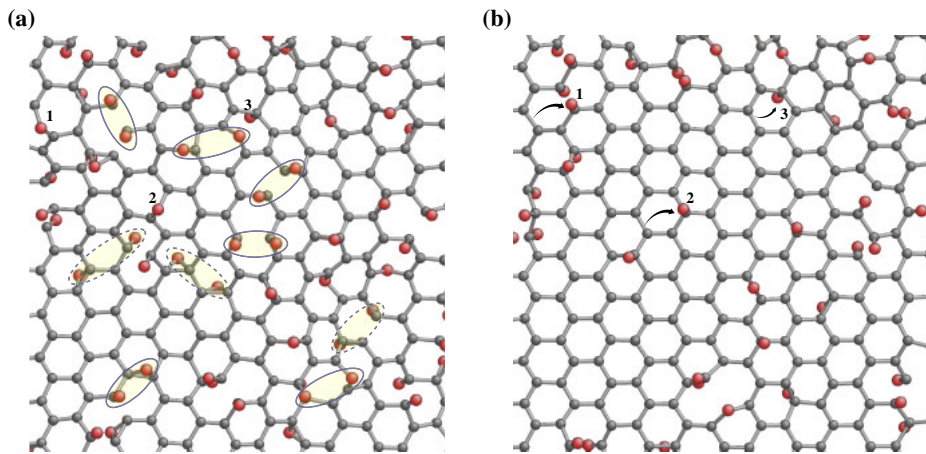


Fig. 4. (Color online) Morphology of GO with 171 (44.53%) first nearest neighboring O pair after (a) relaxation (300 K) and (b) after heat annealing at 1,500 K. The encircled oxygen pairs in (a) indicate the pairs to be released as O_2 gas. The numbered oxygen atom id 1, 2, and 3 are the oxygen atoms moved during reduction and arrows indicate the trajectory of each oxygen atom.

of the numbered oxygen atoms 1, 2 or 3 in Figs. 4(a) and 4(b) are limited in a honeycomb lattice.³⁰⁾ These results show that there was no significant diffusion of oxygen atoms on the basal plane during the reduction process.

In order to confirm the correlation between the initial configuration of epoxides and the magnitude of released O_2 gas molecules, we selected three GO samples with a different density of the first nearest epoxy pairs (37.24,

44.53, and 52.86%). The percentages of released O_2 gas in each case shown in Table I indicate the ratio of the number of released oxygen atoms by a form of O_2 gas/the number of initial oxygen atoms on the GO sheet. In these three cases of GO samples, the number of released O_2 gas/the initial number of first nearest oxygen pair ratio was 22.9% on average. As we assumed that the close proximity of each epoxy pair on the GO sheet affects the amount of

Table I. The results of amount of released O₂ gas from GO sheets consisting of different numbers of first nearest neighboring O pairs (143, 171, and 203) after heat annealing at 1,500 K.

Number of first nearest O pair	Number of released O ₂
143 (37.24%)	26 (6.77%)
171 (44.53%)	42 (11.07%)
203 (52.86%)	52 (13.54%)

released O₂ gas molecules, the results of annealing of each GO sheet show that the magnitude of desorbed O₂ gas has a clear tendency to increase with the higher density of first nearest neighboring epoxy pairs (Table I).

4. Conclusions

Through the observation of the atomic behavior of oxygen functional groups, epoxy, we found that the bond configurations of epoxy groups were rearranged into some different oxygen functional groups, such as ether rings or carbonyls at room temperature. During reduction, such rearranged oxygen functional groups interacted by themselves when they were in close enough proximity. Finally, by comparing reduction results of GO with various densities of first nearest epoxy pairs, we confirmed that the initially high density of epoxy pairs in close proximity increases the magnitude of released O₂ gas molecules.

Acknowledgments

This work was supported by a National Research Foundation (NRF) grant funded by the Korean Government (MEST, No. 2011-0016945) and Basic Science Research Program through the National Research Foundation of Korea (NRF), funded by the Ministry of Education, Science and Technology (No. 2011-0026175).

- 1) H. A. Becerril, J. Mao, Z. Liu, R. M. Stoltberg, Z. Bao, and Y. Chen: *ACS Nano* **2** (2008) 463.
- 2) D. Y. Jeon, K. J. Lee, M. Kim, D. C. Kim, H. J. Chung, Y. S. Woo, and S. Seo: *Jpn. J. Appl. Phys.* **48** (2009) 091601.
- 3) S. Saxena, T. A. Tyson, S. Shukla, E. Negusse, H. Chen, and J. Bai: *Appl. Phys. Lett.* **99** (2011) 013104.
- 4) M. Acik and Y. J. Chabal: *Jpn. J. Appl. Phys.* **50** (2011) 070101.
- 5) I. Jung, D. A. Dikin, R. D. Piner, and R. S. Ruoff: *Nano Lett.* **8** (2008) 4283.
- 6) T. H. Seo, T. S. Oh, S. J. Chae, A. H. Park, K. J. Lee, Y. H. Lee, and E. K. Suh: *Jpn. J. Appl. Phys.* **50** (2011) 125103.
- 7) S. Tanabe, Y. Sekine, H. Kageshima, M. Nagase, and H. Hibino: *Jpn. J. Appl. Phys.* **50** (2011) 04DN04.
- 8) E. Sano and T. Otsuji: *Jpn. J. Appl. Phys.* **48** (2009) 041202.
- 9) A. Lerf, H. He, M. Forster, and J. Klinowski: *J. Phys. Chem. B* **102** (1998) 4477.
- 10) S. Park and R. S. Ruoff: *Nat. Nanotechnol.* **4** (2009) 217.
- 11) S. Saxena, T. A. Tyson, and E. Negusse: *J. Phys. Chem. Lett.* **1** (2010) 3433.
- 12) Y. Zhu, M. D. Stoller, W. Cai, A. Velamakanni, R. D. Piner, D. Chen, and R. S. Ruoff: *ACS Nano* **4** (2010) 1227.
- 13) C. Gómez-Navarro, J. C. Meyer, R. S. Sundaram, A. Chuvalin, S. Kurash, M. Burghard, K. Kern, and U. Kaiser: *Nano Lett.* **10** (2010) 1144.
- 14) D. Yang, A. Velamakanni, C. Bozoklu, S. Park, M. Stoller, R. D. Piner, S. Stankovich, I. Jung, D. A. Field, C. A. Ventrice, Jr., and R. S. Ruoff: *Carbon* **47** (2009) 145.
- 15) K. A. Mkhoyan, A. W. Contrayman, J. Silcox, D. A. Stewart, G. Eda, C. Mattevi, S. Miller, and M. Chhowalla: *Nano Lett.* **9** (2009) 1058.
- 16) C. H. Lucas, A. J. L. Peinado, J. D. L. González, M. L. R. Cervantes, and R. M. M. Aranda: *Carbon* **33** (1995) 1585.
- 17) T. Szabó, O. Berkesi, P. Forgó, K. Josepovits, Y. Sanakis, D. Petridis, and I. Dékány: *Chem. Mater.* **18** (2006) 2740.
- 18) C. Mattevi, G. Eda, S. Agnoli, S. Miller, K. A. Mkhoyan, O. Celik, D. Mastrogiovanni, G. Granozzi, E. Garfunkel, and M. Chhowalla: *Adv. Funct. Mater.* **19** (2009) 2577.
- 19) D. R. Dreyer, S. Park, C. W. Bielawski, and R. S. Ruoff: *Chem. Soc. Rev.* **39** (2010) 228.
- 20) X. Du, I. Skachko, A. Barker, and E. Y. Andrei: *Nat. Nanotechnol.* **3** (2008) 491.
- 21) C. G. Navarro, R. T. Weitz, A. M. Bittner, M. Scolari, A. Mews, M. Burghard, and K. Kern: *Nano Lett.* **7** (2007) 3499.
- 22) A. H. C. Neto, F. Guinea, N. M. R. Peres, K. S. Novoselov, and A. K. Geim: *Rev. Mod. Phys.* **81** (2009) 109.
- 23) G. Eda and M. Chhowalla: *Adv. Mater.* **22** (2010) 2392.
- 24) S. Stankovich, D. A. Dikin, R. D. Piner, K. A. Kohlhaas, A. Kleinhammes, Y. Jia, Y. Wu, S. T. Nguyen, and R. S. Ruoff: *Carbon* **45** (2007) 1558.
- 25) A. B. Bourlinous, D. Gournis, D. Petridis, T. Szabó, A. Szeri, and I. Dékány: *Langmuir* **19** (2003) 6050.
- 26) X. Li, H. Wang, J. T. Robinson, H. Sanchez, G. Diankov, and H. Dai: *J. Am. Chem. Soc.* **131** (2009) 15939.
- 27) H. J. Shin, K. K. Kim, A. Benayad, S. M. Yoon, H. K. Park, I. S. Jung, M. H. Jin, H. K. Jeong, J. M. Kim, J. Y. Choi, and Y. H. Lee: *Adv. Funct. Mater.* **19** (2009) 1987.
- 28) N. Lu, D. Yin, Z. Li, and J. Yang: *J. Phys. Chem. C* **115** (2011) 11991.
- 29) A. Bagri, C. Mattevi, M. Acik, Y. J. Chabal, M. Chhowalla, and V. B. Shenoy: *Nat. Chem.* **2** (2010) 581.
- 30) R. Larciprete, S. Fabris, T. Sun, P. Lacovig, A. Baraldi, and S. Lizzit: *J. Am. Chem. Soc.* **133** (2011) 17315.
- 31) A. C. T. van Duin, S. Dasgupta, F. Lorant, and W. A. Goddard III: *J. Phys. Chem. A* **105** (2001) 9396.